

Astrophysical Implications of a New Dynamical Mass for the Nearby White Dwarf 40 Eridani B

Howard E. Bond,^{1,2} P. Bergeron,³ and A. Bédard³

ABSTRACT

The bright, nearby DA-type white dwarf (WD) 40 Eridani B is orbited by the M dwarf 40 Eri C, allowing determination of the WD’s mass. Until recently, however, the mass depended on orbital elements determined four decades ago, and that mass was so low that it created several astrophysical puzzles. Using new astrometric measurements, the binary-star group at the U.S. Naval Observatory has revised the dynamical mass upward, to $0.573 \pm 0.018 M_{\odot}$. In this paper we use model-atmosphere analysis to update other parameters of the WD, including effective temperature, surface gravity, radius, and luminosity. We then compare these results with WD interior models. Within the observational uncertainties, theoretical cooling tracks for CO-core WDs of its measured mass are consistent with the position of 40 Eri B in the H-R diagram; equivalently, the theoretical mass-radius relation (MRR) is consistent with the star’s location in the mass-radius plane. This consistency is, however, achieved only if we assume a “thin” outer hydrogen layer, with $q_{\text{H}} = M_{\text{H}}/M_{\text{WD}} \simeq 10^{-10}$. We discuss other evidence that a significant fraction of DA WDs have such thin H layers, in spite of expectation from canonical stellar-evolution theory of “thick” H layers with $q_{\text{H}} \simeq 10^{-4}$. The cooling age of 40 Eri B is ~ 122 Myr, and its total age is ~ 1.8 Gyr. We present the MRRs for 40 Eri B and three other nearby WDs in visual binaries with precise mass determinations, and show that the agreement of current theory with observation is excellent in all cases.

Subject headings: astrometry — binaries: visual — stars: fundamental parameters — stars: individual (40 Eridani B) — white dwarfs

¹Department of Astronomy & Astrophysics, Pennsylvania State University, University Park, PA 16802, USA; heb11@psu.edu

²Space Telescope Science Institute, 3700 San Martin Dr., Baltimore, MD 21218, USA

³Département de Physique, Université de Montréal, C.P. 6128, Succ. Centre-Ville, Montréal, QC H3C 3J7, Canada

1. Importance of the 40 Eridani System

The nearby 40 Eridani¹ system has played an important role in astrophysical history, beginning with one of its components being the first white dwarf (WD) to be recognized. The system is a resolved triple, dominated by the fourth-magnitude K0 V star 40 Eri A. The primary lies 83'' from the companion BC binary pair, which currently has a separation of $\sim 8''.3$. The WD component B has a V magnitude of 9.5, and the fainter 40 Eri C is an 11th-mag M4.5 red dwarf.

The story of the recognition of the unusual properties of 40 Eri B in 1910, first by Williamina Fleming, and then by H. N. Russell and E. C. Pickering, was recounted three decades later by Russell (1944). Russell’s parallax measurements had shown the object to be intrinsically faint, yet Fleming found that its spectrum resembled that of a much more luminous A-type star. Within a few years, Adams (1915) showed that the faint companion of Sirius likewise has an A-type spectrum, thus clearly establishing the existence of a new class of underluminous stars with relatively early spectral types. The term “white dwarf” was proposed for these objects by Luyten (1922). Extensive historical details of these early developments are given by Holberg (2007, chapter 2). The modern spectral type of 40 Eri B is DA2.9 (Gianninas et al. 2011, hereafter GBR11), indicating a WD with a hydrogen-dominated photosphere and an effective temperature near 17,000 K.

40 Eri B is the second-brightest WD, outshone only by Sirius B. The revised *Hipparcos* parallax of 200.62 ± 0.23 mas (van Leeuwen 2007) puts the 40 Eri system at a distance of only 4.98 pc, making 40 Eri B the fifth-nearest known WD. Sirius B and Procyon B are closer, but they are much more difficult to observe because of their extremely bright primaries. Van Maanen’s Star (WD 0046+051) and LP 145-141 (WD 1142–645) are also nearer, but are considerably cooler and 2.8 and 1.9 mag fainter. Thus, in many respects, 40 Eri B is the most easily studied of all WDs.

Earlier determinations of the orbital elements of the BC pair were reviewed and updated by van den Bos (1926), who found an orbital period of approximately 248 yr—based on observations covering only $\sim 58\%$ of the period, including low-accuracy data from the late 18th and early 19th centuries. Van den Bos estimated the mass of B to be about $0.44 M_{\odot}$. Nearly five decades later, Heintz (1974, hereafter H74) analyzed a half-century of additional astrometric observations, but found a similar period of 252 yr and a mass of $0.43 \pm 0.02 M_{\odot}$ for the WD. This mass determination was based on an adopted absolute parallax of 207 ± 2 mas.

¹The Bayer designation is omicron-2 (\omicron^2) Eridani, but it is used less frequently, probably because of the inconvenient superscript. The system is cataloged as GJ 166. 40 Eri B is also designated WD 0413–077 in the white-dwarf literature.

2. Astrophysical Puzzles of a Low Mass

A dynamical mass of 40 Eri B as low as the $0.43 M_{\odot}$ found by H74 creates several astrophysical issues. For example, Iben & Tutukov (1986) and Iben (1987) stated that the lowest possible mass of a WD that can be formed through single-star evolution at the present age of the Universe is $\sim 0.50 M_{\odot}$. This led them to suggest—assuming the H74 mass to be correct—that 40 Eri B is a helium-core WD that resulted from a binary-star merger. However, as shown by Provencal et al. (1998, their Figure 1), the position of 40 Eri B in the theoretical mass-radius plane for a mass of $0.43 M_{\odot}$ requires a core composed of nuclei of atomic weights between those of magnesium and iron—an apparent astrophysical impossibility.

Shipman et al. (1997, hereafter SPHT97) and Provencal et al. (1998) used the then recently available *Hipparcos* parallax (198.24 ± 0.84 mas) to revise H74’s dynamical mass upward to $0.501 \pm 0.011 M_{\odot}$ —barely sufficient to remove the discrepancy with single-star evolution, but implying an extremely large age for the 40 Eri system. However, the dynamical mass drops back down to $0.481 \pm 0.015 M_{\odot}$ if we combine the 2007 revised *Hipparcos* parallax mentioned above with the H74 orbital elements.

Koester & Weidemann (1991, hereafter KW91) measured the gravitational redshift (GR) of 40 Eri B. Combining this with the inferred radius of the star, KW91 concluded that the GR implied a mass of $0.53 \pm 0.04 M_{\odot}$. This higher mass was more consistent with the expected mass-radius relation (MRR) for WDs with carbon-oxygen cores than the dynamical mass derived from the visual orbit. The GR was measured again a few years later by Reid (1996), who also made a new determination of the radius, but it resulted in a similar mass of $0.522 \pm 0.029 M_{\odot}$.

Over the next two decades, investigators of 40 Eri B continued to cite masses derived from the H74 orbital elements. For example, Holberg et al. (2012) quoted the dynamical mass of $0.501 \pm 0.011 M_{\odot}$ from SPHT97, and stated that it agreed well with the mass implied by the GR. By comparing the location of 40 Eri B in the mass-radius plane with theoretical models for CO-core WDs with thick and thin hydrogen envelopes, they concluded—as had KW91—that the relatively low mass provides “strong evidence” for a thin envelope (i.e., $q_{\text{H}} \simeq 10^{-10}$, where $q_{\text{H}} = M_{\text{H}}/M_{\text{WD}}$ is the ratio of the mass of the surface hydrogen layer to the mass of the star).

Based on a model-atmosphere analysis of 40 Eri B, from which the effective temperature, surface gravity, and radius were derived, and using an adopted theoretical MRR, Giammichele et al. (2012) obtained an even higher mass of $0.59 \pm 0.03 M_{\odot}$. Since the techniques used to derive this mass are widely used in discussions of the WD mass distribution

function, the apparent discrepancy with a directly measured dynamical mass for one of the best-known and brightest WDs is of considerable concern.

3. A New Dynamical Mass

Given the importance of 40 Eri B for WD astrophysics, we were surprised that the visual orbit had not been updated with new observations over the more than four decades since H74. We contacted the binary-star group at the United States Naval Observatory (USNO), which maintains the Washington Double Star Catalog (WDS; Mason et al. 2001), a compilation of all published astrometric measurements of visual binaries. In response, the USNO group assembled all of the data on 40 Eri BC contained in the WDS. We also provided them with a precise measurement based on archival *Hubble Space Telescope* (*HST*) images obtained in 2006. Moreover, and crucially, in early 2017 they obtained two new high-precision observations with the speckle camera on the 26-inch telescope at the USNO in Washington, DC. From these sources there are 22 new measurements since the last one listed by H74, covering 1974.8 to 2017.2—as well as 158 earlier observations between 1851.1 and 1973.8.

Using these data, Mason et al. (2017, hereafter MHM17) have computed updated elements for the 40 Eri BC orbit, leading to a significant revision of the dynamical masses. Although the semi-major axis is nearly unchanged from H74, the new elements lead to a reduction in the orbital period to $P = 230.29 \pm 0.68$ yr—a 20% increase in P^{-2} , and thus in the masses, compared to H74. The new dynamical mass for 40 Eri B based on the MHM17 analysis and the 2007 *Hipparcos* parallax is $0.573 \pm 0.018 M_{\odot}$.

In the remainder of this paper, we will also re-evaluate other parameters of the WD, and then discuss the astrophysical implications of these new results.

4. Astrophysical Parameters of 40 Eri B

The most precise method to determine the atmospheric parameters (T_{eff} and $\log g$) of DA WDs is the spectroscopic technique (Bergeron et al. 1992, hereafter BSL92; Liebert et al. 2005, hereafter LBH05; GBR11), wherein the observed Balmer line profiles are compared with predictions of modern model atmospheres using χ^2 minimization. The model atmospheres and synthetic spectra we use are similar to the pure-hydrogen LTE models described in Tremblay & Bergeron (2009, and references therein). In the case of 40 Eri B, the atmosphere is purely radiative, and thus the solution does not depend on uncertainties in the

treatment of convective energy transport. As described in §2 (and in BSL92, their §6.4), 40 Eri B, with a directly measured dynamical mass, is a key object to test the validity of the spectroscopic technique.

We have available nine high signal-to-noise, medium-resolution (~ 6 Å FWHM) spectra of 40 Eri B obtained over the past 25 years, mostly with the Steward Observatory 2.3-m telescope at Kitt Peak; details of these spectra are given by GBR11. The individual spectroscopic determinations of T_{eff} and $\log g$ from these spectra are plotted in Figure 1. The standard deviations (combined in quadrature with the formal internal errors of the fits) are $\sigma(T_{\text{eff}}) = 220$ K and $\sigma(\log g) = 0.036$, which are represented by the 1σ and 2σ ellipses in Figure 1. These dispersions are similar to the typical external errors of 1.4% in T_{eff} and 0.042 dex in $\log g$ found by LBH05 in fitting DA spectra (values corrected by Bédard et al. 2017 for a minor error in LBH05). By averaging the values from all our spectra, and calculating the corresponding errors on the mean, we find a final result of $T_{\text{eff}} = 17,200 \pm 110$ K and $\log g = 7.957 \pm 0.020$.

Using these atmospheric parameters, we can now determine the radius of 40 Eri B, following the approach described in detail in Bédard et al. (2017). Briefly, measured stellar magnitudes—Johnson-Kron-Cousins $BVRI$, Strömgren $ubvy$, and 2MASS JHK_s —are converted into absolute fluxes, using appropriate photometric zero-points. These are then compared with model fluxes integrated over the same filter bandpasses. The solid angle, $\pi(R/D)^2$, where R is the radius of the star and D its distance from Earth, is considered a free parameter, with T_{eff} set at the spectroscopic value. The distance D is known to 0.1% uncertainty from the revised *Hipparcos* trigonometric parallax (§1). We obtain $R = 0.01308 \pm 0.00020 R_{\odot}$. Combining this with the spectroscopic $\log g$ value yields an expected mass of $0.565 \pm 0.031 M_{\odot}$, in excellent agreement with the directly measured dynamical mass. The luminosity of 40 Eri B from these parameters is $0.01349 \pm 0.00054 L_{\odot}$.

5. Comparisons with White-Dwarf Theory

We now make comparisons of the new measured parameters of 40 Eri B with theoretical WD cooling tracks and MRRs, and with the predicted GR. For the cooling tracks, we use theoretical modeling data from the “Montréal” tables² for WDs with carbon-oxygen cores surrounded by helium layers with a mass of 1% of the stellar mass. WDs with thick ($q_{\text{H}} = 10^{-4}$) and thin ($q_{\text{H}} = 10^{-10}$) hydrogen layers will be considered.

²Available at <http://www.astro.umontreal.ca/~bergeron/CoolingModels>.

The two panels in Figure 2 show the location of 40 Eri B in the theoretical Hertzsprung-Russell diagram (HRD; luminosity vs. effective temperature). Also plotted are the model cooling tracks for WDs with masses of 0.5, 0.6, 0.7, and 0.8 M_{\odot} . In the top panel, the tracks are for thick H layers, and in the bottom panel they are for thin H layers. The position of the star in the HRD can be used to infer its mass, independently of any actual direct measurement of the mass. As discussed in the caption of Figure 2, we find an excellent agreement of the predicted mass of the star with the measured dynamical mass by assuming a thin H layer.

In Figure 3 we plot the MRRs for CO-core WDs from the Montréal tables, interpolated to an effective temperature of 17,200 K, for both thick and thin H layers. To illustrate the dependence on the mean molecular weight of the core, we also plot the MRR for zero-temperature WDs with an iron core, from Hamada & Salpeter (1961). The blue filled circle with error bars shows the location of 40 Eri B, based on the radius from §4, and the dynamical mass from MHM17. Its location clearly indicates a thin H layer, in agreement with the inference from its position in the HRD.

For our value of the radius and the new dynamical mass, the predicted GR is $27.82 \pm 0.97 \text{ km s}^{-1}$. This agrees within the quoted errors with the values of $26.5 \pm 1.5 \text{ km s}^{-1}$ measured by KW91³ and $25.8 \pm 1.4 \text{ km s}^{-1}$ reported by Reid (1996).

6. Discussion

The apparent low mass of the WD 40 Eri B, based on orbital elements determined more than four decades ago, gave rise to several puzzles, as outlined in §2. The modern dynamical mass presented by MHM17 is $\sim 20\%$ higher, and appears to resolve most of the astrophysical

³KW91 give sufficient details of their analysis for us to make the following comments. The GR of 26.5 km s^{-1} that they reported was based on a measured radial-velocity (RV) difference of 28.8 km s^{-1} between the sharp absorption core of H α in 40 Eri B and the strong H α emission line in 40 Eri C (corrected for the GR of C), adjusted by 2.3 km s^{-1} for the relative orbital motion of B with respect to C, according to the H74 orbital elements. Using our new elements, the RV difference at the date of the KW91 observation was slightly different, 2.8 km s^{-1} ; however, although KW91 did not point this out, the sign of this adjustment is unknown, giving a GR of either 26.0 or 31.6 km s^{-1} . Alternatively, KW91 also measured the RV of B relative to 40 Eri A, from several absorption lines in the latter, to be 28.0 km s^{-1} . This has to be corrected for the velocity of B relative to the center of mass of the BC system, 0.7 km s^{-1} (again with unknown sign) according to the new elements. Neglecting the motion of A relative to BC, this gives either 27.3 or 28.7 km s^{-1} , both of which agree quite well with the expected GR of 27.8 km s^{-1} from the new radius and mass.

issues. In this section we discuss some of the further implications of the revised mass.

6.1. The Thin Hydrogen Layer

Modern theories of post-asymptotic-giant-branch (post-AGB) evolution predict WDs to have thick hydrogen layers of about $q_{\text{H}} \simeq 10^{-4}$ to 10^{-5} , depending on the progenitor mass (e.g., Althaus et al. 2010). However, there is considerable evidence, based on spectral evolution of WDs, that many DA stars may have H layers much thinner than this canonical value (see Fontaine & Wesemael 1987, 1997 for reviews): (1) Along the cooling sequence of WDs, there is a range in effective temperatures, $T_{\text{eff}} \simeq 45,000$ – $30,000$ K, in which nearly all WDs are of the DA type. The existence of this “DB gap” can be explained in terms of a float-up model, in which traces of H, which is thoroughly diluted within the thick helium-rich envelope of a hot DO star, slowly diffuse up to the surface, gradually transforming the DO progenitor into a DA WD by the time it reaches the hot edge of the gap near 45,000 K. Then at the cool edge near 30,000 K, DA WDs with H layers that are thin enough, $q_{\text{H}} \lesssim 10^{-15}$, are expected to transform back into DB stars through the dilution of the thin radiative hydrogen atmosphere by the deeper and more massive convective helium envelope (MacDonald & Vennes 1991). About 20% of DA WDs appear to have H layers this thin. (2) A further significant increase in the ratio of non-DA to DA WDs to about unity is observed below $T_{\text{eff}} \simeq 10,000$ K, most likely resulting from the convective mixing of the superficial H layer with the deeper He envelope. This directly implies that about half of DA stars must have hydrogen layers with $q_{\text{H}} \lesssim 10^{-6}$ (Tremblay & Bergeron 2008, hereafter TB08). In principle, asteroseismological studies of ZZ Ceti stars can provide a direct measurement of the thickness of the H layer in pulsating DA WDs, but reliable measurements are only available for a few stars (e.g., Giammichele et al. 2016 and references therein).

As discussed in §5, the precise dynamical mass measured for 40 Eri B provides evidence for a thin H layer, consistent with the picture just outlined in which many DA WDs have such thin layers. Our finding is significant at a level of about 2σ , as indicated by the error bars in Figure 3. At present, the star remains a DA WD; but as it cools the bottom of the H convection zone will eventually reach the underlying and much more massive convective helium envelope, resulting in a mixing of the H and He layers. This will turn the DA star into a helium-atmosphere WD—a DC star in this case—with at most a weak detectable $\text{H}\alpha$ absorption feature. Since the bottom of the H convection zone reaches deeper as T_{eff} decreases (see TB08, their Figure 1), the temperature at which this mixing process will occur is a function of the H layer’s mass: for thicker hydrogen layers, the mixing occurs at lower effective temperatures. A DA star with a thin H layer of $q_{\text{H}} = 10^{-10}$ would mix at

$T_{\text{eff}} \simeq 10,000$ K. However, although our results indicate that 40 Eri B possesses a thin H layer, it is not possible to constrain the layer’s mass very precisely, and thus the temperature at which its spectral type will change is uncertain.

There are wider implications if many DA WDs have thin H layers. Studies of the mass distributions for DA stars have generally relied on spectroscopic $\log g$ determinations similar to that described here for 40 Eri B, and then the mass is inferred from a MRR. Usually these analyses adopt CO-core models with an assumption of thick H layers. The adopted thickness of the H layer directly affects the derived mass, in the sense that assuming more massive H layers yields larger spectroscopic masses (see BSL92, their §3.4, and our Figures 2 and 3). The shift in derived stellar mass by going from no H layer to a thick one is $\sim 0.026 M_{\odot}$ for WDs in the ZZ Ceti instability strip (Bergeron et al. 1995), and the effect is greater for hotter and/or lower-mass stars (e.g., LBH05). At the temperature of 40 Eri B, the shift is $\sim 0.036 M_{\odot}$ (our Figure 3).

6.2. Age and Past Evolution of the System

Isochrones are plotted in the HRD in Figure 2. They imply a cooling age of 40 Eri B of about 122 Myr, assuming a thin H layer. Using an initial-final mass relation given by Salaris et al. (2009) that applies to WDs near the low-mass end of their mass distribution, $M_{\text{final}} = 0.134M_{\text{initial}} + 0.331$, we can infer that the initial mass of the progenitor of 40 Eri B was about $1.8 M_{\odot}$. The pre-WD lifetime of such a star is about 1.7 Gyr, giving a total age of the system of ~ 1.8 Gyr. Thus earlier concerns about an excessive age (§2) appear to be resolved.

In the present-day orbit, the periastron separation of B and C is 19.7 AU. Under the assumption that the mass loss from the progenitor of B was isotropic and on a timescale long compared to the orbital period (cf. Burleigh et al. 2002, §2), and ignoring any interactions between the stars, this implies that the periastron separation was only ~ 6.3 AU in the progenitor BC binary. Thus the system probably avoided Roche-lobe overflow when the progenitor of B was an AGB star. However, the M dwarf was certainly deeply embedded in the outflowing AGB wind, and may have accreted significant mass and angular momentum. Thus it is perhaps surprising that it has no apparent chemical peculiarities, such as an enhanced carbon abundance. These points have been discussed by Fuhrmann et al. (2014), who suggested that the chromospheric activity of the flare star 40 Eri C may be due to it having been spun up to a higher rotational velocity by accretion during the AGB phase of B.

It is also surprising that the eccentricity of the 40 Eri BC orbit remained high (0.43; see

MHM17), in spite of the significant tidal interactions that likely occurred during the AGB phase. This ought to have led to some circularization of the orbit. The situation is reminiscent of the systems of Procyon and Sirius, which also contain WDs orbiting the primary stars with eccentricities of 0.40 and 0.59, respectively, in spite of periastron separations of only a few AU in the progenitor systems. Possible explanations, involving eccentricity-pumping during the AGB phase, were reviewed by Bond et al. (2017) in their discussion of Sirius.

6.3. Mass-Radius Relation for White Dwarfs in Nearby Visual Binaries

In the immediate solar neighborhood there are four canonical visual binaries containing WD components. They provide the best available observational constraints on the MRR (along with WDs in close post-common-envelope eclipsing binaries—e.g., O’Brien et al. 2001; Parsons et al. 2017 and references therein). The revised mass for 40 Eri B discussed in this paper now joins the very precise dynamical masses for Procyon B and Sirius B, recently obtained through long-term astrometric programs with *HST* (Bond et al. 2015, 2017). The fourth nearby WD in a visual binary is Stein 2051 B. In this case, an earlier approximate dynamical mass determination for this wide binary (Strand 1977) has recently been supplanted by a determination of its mass from the relativistic deflection of a background star’s image as Stein 2051 B passed in front of it (Sahu et al. 2017). Effective temperatures, luminosities, and radii for these four WDs have been determined using photometric techniques similar to those described above (§4), and the data and literature references are presented in Table 1.

In Figure 4 we plot the MRRs for these four WDs. For each object, we interpolated in the Montréal tables to obtain the relations for WDs with the corresponding effective temperatures. For Sirius B, we assumed a thick H layer. For the helium-atmosphere WDs Procyon B and Stein 2051 B, we used the thin H layer relations, which are a good approximation for DB WDs and related objects. A thin H layer was also adopted for 40 Eri B, as discussed above. The four MRRs are color-coded to match the corresponding observed data points. As Figure 4 shows, the agreement of the theoretically modeled relations with the measurements is excellent.

6.4. Conclusion

A new dynamical mass has been determined at the USNO for the nearby, important WD 40 Eri B. We have also updated its atmospheric parameters. We compared the observations with modern theoretical HRDs and MRRs, and showed that the theory predicts the

luminosity and radius well within the observational uncertainties, provided that we assume a CO-core WD with a thin H layer. We also compared theoretical MRRs with the data for three other nearby WDs in visual binaries with recently well-determined masses, and again found good agreement. Our findings support a picture in which a significant fraction of DA WDs have thin H layers. If so, this implies that the mass distribution function for DA WDs will have to be shifted downward by a few hundredths of a solar mass.

We thank the USNO double-star team—Brian Mason, William Hartkopf, and Korie Miles—for their quick response to our inquiry, and for communicating their important update of the 40 Eri B dynamical mass in advance of publication. This work was supported in part by the NSERC Canada and by the Fund FRQ-NT (Québec).

REFERENCES

- Adams, W. S. 1915, *PASP*, 27, 236
- Althaus, L. G., Córscico, A. H., Bischoff-Kim, A., et al. 2010, *ApJ*, 717, 897
- Bédard, A., Bergeron, P., & Fontaine, G. 2017, *ApJ*, submitted
- Bergeron, P., Saffer, R. A., & Liebert, J. 1992, *ApJ*, 394, 228 (BSL92)
- Bergeron, P., Wesemael, F., Lamontagne, R., et al. 1995, *ApJ*, 449, 258
- Bond, H. E., Gilliland, R. L., Schaefer, G. H., et al. 2015, *ApJ*, 813, 106
- Bond, H. E., Schaefer, G. H., Gilliland, R. L., et al. 2017, *ApJ*, 840, 70
- Burleigh, M. R., Clarke, F. J., & Hodgkin, S. T. 2002, *MNRAS*, 331, L41
- Fontaine, G., & Wesemael, F. 1987, *The Second Conference on Faint Blue Stars (IAU Colloq. 95)*, ed. A. G. D. Philip, D. S. Hayes, & J. Liebert (Schenectady, NY: Davis), 319
- Fontaine, G., & Wesemael, F. 1997, *White Dwarfs*, ed. J. Isern, M. Hernanz, & E. García-Berro (Dordrecht: Kluwer), 173
- Fuhrmann, K., Chini, R., Buda, L.-S., & Pozo Nuñez, F. 2014, *ApJ*, 785, 68
- Giammichele, N., Bergeron, P., & Dufour, P. 2012, *ApJS*, 199, 29
- Giammichele, N., Fontaine, G., Brassard, P., & Charpinet, S. 2016, *ApJS*, 223, 10
- Gianninas, A., Bergeron, P., & Ruiz, M. T. 2011, *ApJ*, 743, 138 (GBR11)
- Hamada, T., & Salpeter, E. E. 1961, *ApJ*, 134, 683
- Heintz, W. D. 1974, *AJ*, 79, 819 (H74)
- Holberg, J. B. 2007, *Sirius: Brightest Diamond in the Night Sky* (Berlin: Springer)
- Holberg, J. B., Oswalt, T. D., & Barstow, M. A. 2012, *AJ*, 143, 68
- Iben, I., Jr. 1987, *Mem. Soc. Astron. Italiana*, 58, 131
- Iben, I., Jr., & Tutukov, A. V. 1986, *ApJ*, 311, 753
- Koester, D., & Weidemann, V. 1991, *AJ*, 102, 1152 (KW91)
- Liebert, J., Bergeron, P., & Holberg, J. B. 2005, *ApJS*, 156, 47 (LBH05)
- Luyten, W. J. 1922, *PASP*, 34, 356
- MacDonald, J., & Vennes, S. 1991, *ApJ*, 371, 719
- Mason, B. D., Hartkopf, W. I., & Miles, K. N. 2017, arXiv:1707.03635 (MHM17)
- Mason, B. D., Wycoff, G. L., Hartkopf, W. I., Douglass, G. G., & Worley, C. E. 2001, *AJ*, 122, 3466

- O'Brien, M. S., Bond, H. E., & Sion, E. M. 2001, *ApJ*, 563, 971
- Parsons, S. G., Gänsicke, B. T., Marsh, T. R., et al. 2017, *MNRAS*, 470, 4473
- Provencal, J. L., Shipman, H. L., Høg, E., & Thejll, P. 1998, *ApJ*, 494, 759
- Provencal, J. L., Shipman, H. L., Koester, D., Wesemael, F., & Bergeron, P. 2002, *ApJ*, 568, 324
- Reid, I. N. 1996, *AJ*, 111, 2000
- Russell, H. N. 1944, *AJ*, 51, 13
- Sahu, K. C., Anderson, J., Casertano, S., et al. 2017, *Science*, 356, 1046
- Salaris, M., Serenelli, A., Weiss, A., & Miller Bertolami, M. 2009, *ApJ*, 692, 1013
- Shipman, H. L., Provencal, J. L., Høg, E., & Thejll, P. 1997, *ApJ*, 488, L43 (SPHT97)
- Strand, K. A. 1977, *AJ*, 82, 745
- Tremblay, P.-E., & Bergeron, P. 2008, *ApJ*, 672, 1144 (TB08)
- Tremblay, P.-E., & Bergeron, P. 2009, *ApJ*, 696, 1755
- van den Bos, W. H. 1926, *Bull. Astron. Inst. Netherlands*, 3, 128
- van Leeuwen, F. 2007, *A&A*, 474, 653

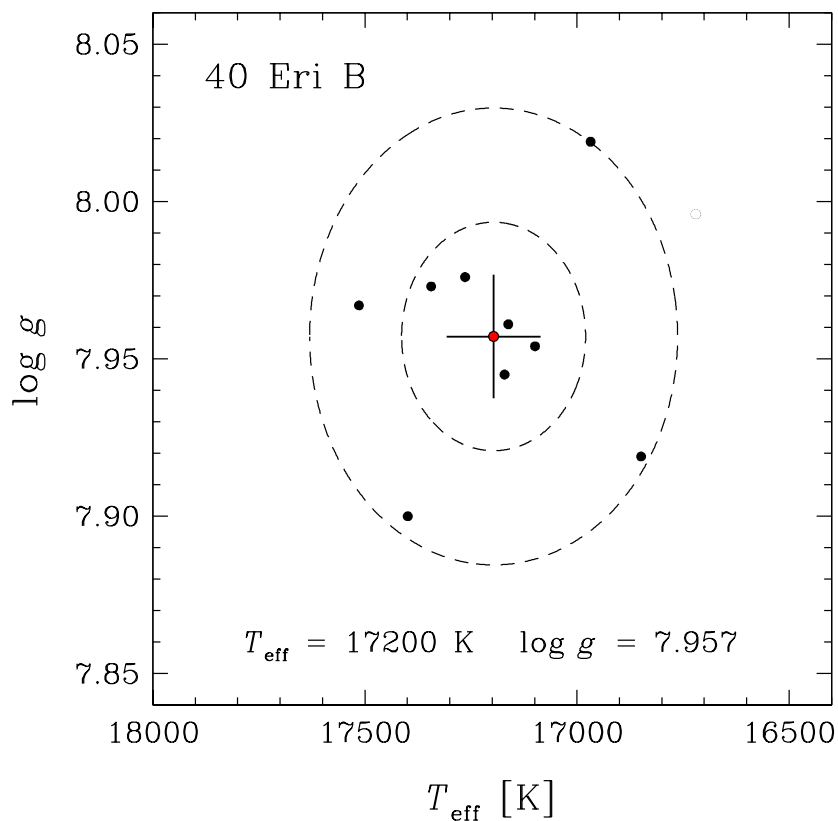


Fig. 1.— Spectroscopic determinations of T_{eff} and $\log g$ for 40 Eri B, based on nine independent spectroscopic observations (*black filled circles*). The ellipses represent the 1σ and 2σ dispersions, including the formal internal errors of the fits, with $\sigma_{T_{\text{eff}}} = 220 \text{ K}$ and $\sigma_{\log g} = 0.036$. The average values are given in the figure and indicated by the red filled circle, whose error bars represent the errors on the mean values, $T_{\text{eff}} = 17,200 \pm 110 \text{ K}$ and $\log g = 7.957 \pm 0.020$.

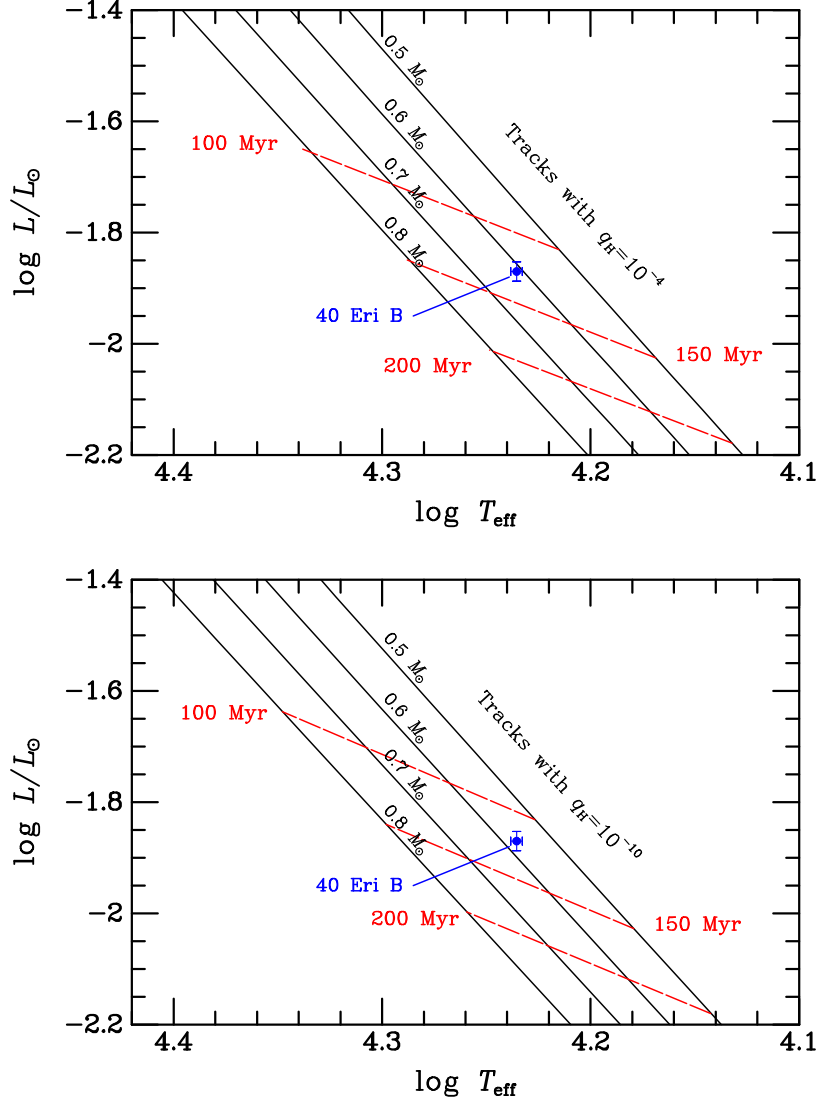


Fig. 2.— Comparisons of theoretical white-dwarf cooling tracks with the observed position of 40 Eri B in the H-R diagram (*filled blue circles* in both panels). **Top:** Cooling tracks (*black lines*) and isochrones (*dashed red lines*) for CO-core white dwarfs of the indicated masses with “thick” hydrogen layers ($q_{\text{H}} = 10^{-4}$). The implied mass of 40 Eri B is $0.611 M_{\odot}$, in poor agreement with the measured $0.573 M_{\odot}$. **Bottom:** Cooling tracks and isochrones for CO-core white dwarfs with “thin” hydrogen layers ($q_{\text{H}} = 10^{-10}$). Now the implied mass is $0.572 M_{\odot}$, in excellent accord with the measured dynamical mass. The inferred cooling age is 122 Myr.

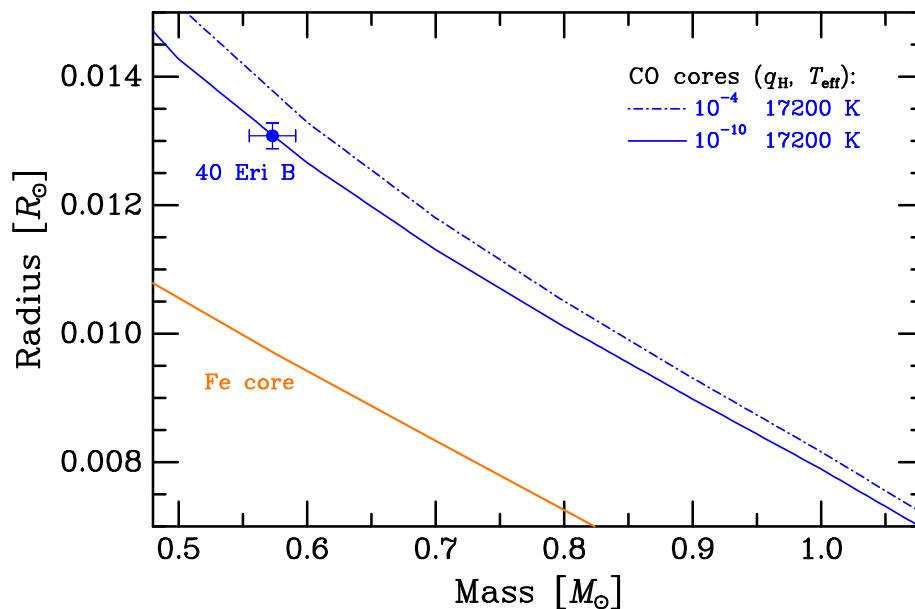


Fig. 3.— Observed position of 40 Eri B in the mass-radius plane (*filled blue circle*), compared with theoretical relations from the Montréal database for CO-core white dwarfs of effective temperature $T_{\text{eff}} = 17,200$ K. The *dash-dot blue line* shows the relation for a thick H layer, and the *solid blue line* is for a thin H layer. Also plotted (*orange line*) is the Hamada–Salpeter mass-radius relation for a zero-temperature white dwarf composed of iron. The agreement of theory with the observations of 40 Eri B is excellent for a thin H layer CO-core white dwarf.

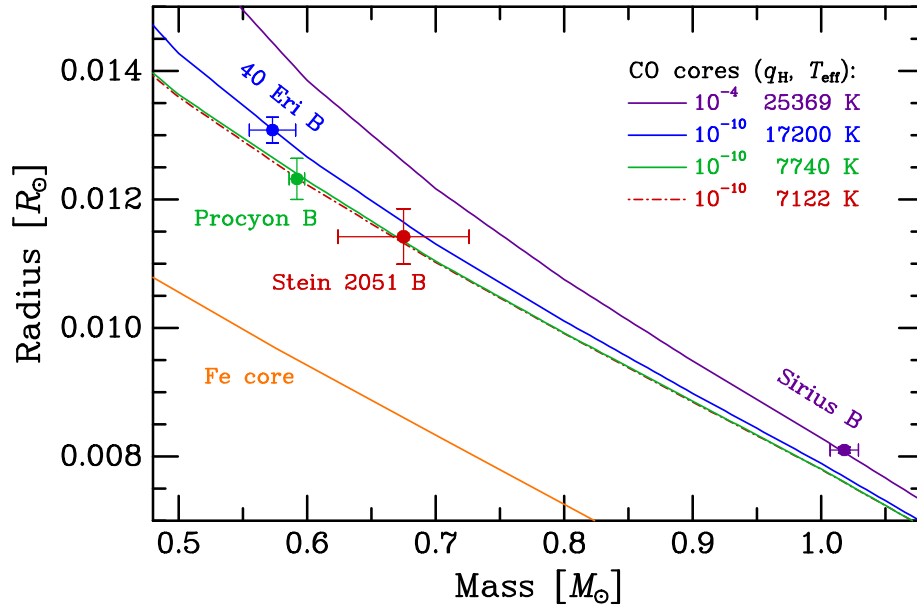


Fig. 4.— Positions in the mass-radius plane of four white dwarfs in visual binaries (*filled circles*), compared with theoretical relations appropriate for the H layer thickness and effective temperature of each star (*lines*). The plotted points and lines use a different color-code for each star. In each case the theoretical relation agrees within the uncertainties with the corresponding observation. (This figure is an updated version of one that appeared in Sahu et al. 2017.)

Table 1. Astrophysical Parameters for White Dwarfs in Nearby Visual Binaries

Star	Sp. Type	T_{eff} [K]	Ref.	Radius [R_{\odot}]	Ref.	Mass ^a [M_{\odot}]	Ref.
Procyon B	DQZ	7740 ± 50	1	0.01232 ± 0.00032	1, 5	0.592 ± 0.006	5
Sirius B	DA2	$25,369 \pm 46$	2	0.008098 ± 0.000046	2	1.018 ± 0.011	2
Stein 2051 B	DC	7122 ± 181	3	0.0114 ± 0.0004	3	0.675 ± 0.051	3
40 Eri B	DA2.9	$17,200 \pm 110$	4	0.01308 ± 0.00020	4	0.573 ± 0.018	6

^aDynamical masses from binary orbits for Procyon B, Sirius B, and 40 Eri B; from the relativistic deflection of a background star image for Stein 2051 B (see text).

References. — (1) Provencal et al. 2002; (2) Bond et al. 2017; (3) Sahu et al. 2017; (4) This paper; (5) Bond et al. 2015; (6) Mason et al. 2017.